Structural Eng./Earthquake Eng., JSCE, Vol.22, No. 2, 159s-166s, 2005 October
(Translated from a paper which originally appeared on Journal of Applied Mechanics, JSCE, Vol.6, pp.993-1000, 2003.8)

# FBG-BASED VIBRATION SENSOR USING GRAVITY EFFECTS FOR LARGE INFRASTRUCTURES

Hiroki KAZAMA[1] and Akira MITA[2]

[1] Graduate Student , Dept. of System Design Eng., Keio University
(3-14-1 Hiyoshi, Kohoku-ku, Yokohama 223-8522, Japan)
E-mail:hiroki-k@kitanet.ne.jp
[2] Professor, Dept. of System Design Eng., Keio University
(3-14-1 Hiyoshi, Kohoku-ku, Yokohama 223-8522, Japan)
E-mail:mita@sd.keio.ac.jp

A simple mechanism for a vibration sensor based on fiber Bragg grating (FBG) is proposed. The mechanism utilizes the gravity force to allow the maximum sensitivity of the sensor into vertical direction while the minimum sensitivity for other two transverse directions. The sensor consists of a FBG cable and several masses to form a vibration system. The cable is extended to introduce a certain tensile force and acts as a spring. The sensitivity of the sensor is more than 1 μstrain/gal for vertical direction. This simple sensor has been developed for damage detection of large structures. Several prototypes were fabricated. And extensive shaking table tests were conducted to examine the performance.

***Key Words :*** *FBG accelerometer, vibration sensor, smart infrastructure*

## 1. INTRODUCTION

Important infrastructures such as bridges and pipelines need routine checkup for keeping their good functionality. However, the checkup solely depending of humans has certain limitations on the accuracy and the accessibility. In addition, the costs associated with the checkup are also high. Recently many fiber optic sensors have been proposed and developed. They have many advantages to change the human-based checkup to automatic systems. One of the most promising fiber optic sensors is fiber Bragg grating (FBG). However, the measurement of vibration using FBG may need mechanical apparatuses that transfer the vibration values into uniform strain induced in the FBG element. Thus, the purpose of the study is to propose a simple mechanism for FBG vibration sensors that ensure the uniform strain distribution in the FBG element.

## 2. MECHANISM

### (1) Principle of FBG

FBG is the optical fiber which is given the periodic refractive-index change to the core. If the refractive index of a core is $n$ and the interval of the Bragg Grating is $d$, when broad band light is applied to the FBG section, it reflects only the wavelength λ determined by the Equation 1. Therefore, the strain and the temperature arising at the FBG section can be measured by observing the wavelength of the reflective light.

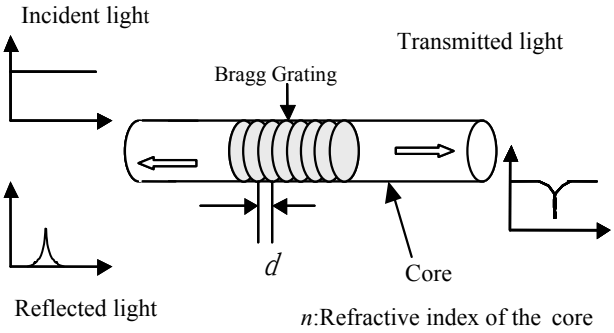


**Fig. 1** Schematic diagram of FBG.

$$\lambda = 2nd \tag{1}$$

### (2) Principle of FBG vibration sensor

Several FBG vibration sensors have been developed, aiming at high accuracy in relatively low freq-

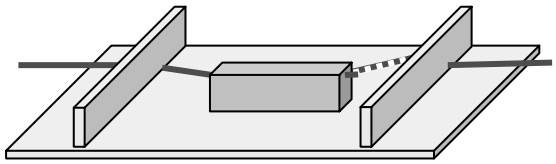

**Fig. 2** FBG vibration sensor using gravity effects (Concentrated mass).

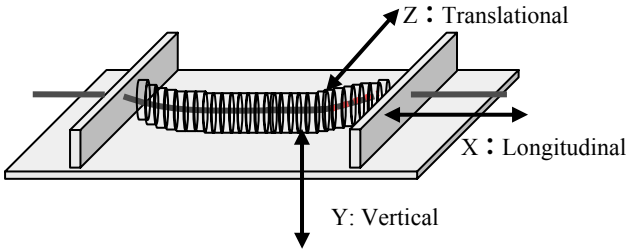


**Fig. 3** FBG vibration sensor using gravity effects (Distributed mass).

uency band, and avoiding the influence of a cross talk. However the mechanism of the sensors are relatively complicated[1),2)] . Kanda and Mita proposed a new mechanism for FBG vibration sensor using gravity effect[3)]shown in the **Fig. 2**. They showed the possibility of a small-sized sensor, reduction of cost, and high sensitivity. The features of the sensor are as follows.

It employs a simple mechanism. A mass is attached to the center of an optical fiber stretched along the frame. Due to the sag arising from the gravity, it has excellent sensitivity in the vertical direction, while very low sensitivity in other two perpendicular directions.

High sensitivity is realized by using resonance. However, the following problems remain.Strong shear force arising at the edge of the mass sometimes causes breaks in the optical fiber.Undesirable modes are excited by eccentricity of the gravity center of the mass.

In this paper, in order to resolve the above problems, a FBG vibration sensor using gravity effects and distributed mass over the optical fiber is proposed. The distributed mass continues till the edge of the fiber. **Fig. 3** shows the prototype mechanism of proposed sensor. The rectangular coordinates system is also depicted in **Fig. 3**.

**(3) Sensitivity of distributed mass sensor**

Many advantages can be achieved by changing the mass to the distributed configuration. However, the sensitivity of the distributed mass sensor may be reduced compared to the concentrated mass sensor. Constructing the static equation of equilibrium, the relation between the number of division and sensitivity can be derived. The magnitude of the reduction in the sensitivity is shown in **Fig. 4**. with respect to the number of division, N. Parameters are :

$m_k$: the $k$-th mass
$g$: gravitational constant
$E$: young's modulus of the optical fiber
$A$: cross-sectional area of optical fiber
$\varepsilon_i$: strain of $i$-th optical fiber form the left
$L_0$: distance between neighboring masses
$L_{all}$: total length of the sensor

**Fig. 5** shows the state of the sensor with gravity. **Fig. 6** shows $i$-th section of the sensor.
The strain arising at the $i$-th section of the optical fiber can be related to the strain arising at the center $\varepsilon_{N/2}$.

$$\varepsilon_i = \sqrt{\varepsilon_{N/2+1}{}^2 + \left(\sum_{k=i}^{N/2} \frac{m_k g}{EA}\right)^2} \tag{2}$$

The first term in the root indicates the squared horizontal strain, and the second term the squred vertical strain. Therefore, the angle of the optical fiber $\theta$ isexpressed as

$$\sin\theta = \frac{\sum_{k=i}^{N/2} \frac{m_k g}{EA}}{\sqrt{\varepsilon_{N/2+1}{}^2 + \left(\sum_{k=i}^{N/2} \frac{m_k g}{EA}\right)^2}}$$
$$\cos\theta = \frac{\varepsilon_{N/2+1}}{\sqrt{\varepsilon_{N/2+1}{}^2 + \left(\sum_{k=i}^{N/2} \frac{m_k g}{EA}\right)^2}} \tag{3}$$

Using the above results, the horizontal length of the optical fiber of one section $L_i$, shown in the **Fig. 6**, is obtained as,

$$L_i = \left(1 + \sqrt{\varepsilon_{N/2+1}{}^2 + \left(\sum_{k=i}^{N/2} \frac{m_k g}{EA}\right)^2}\right) L_0 \cos\theta \tag{4}$$

The sum of $L_i$ ($i$=1,N) must be equal to the length of the sensor when it does not have masses. The fiber is stretched to introduce the initial tensile strain characterized by the prestrain $\varepsilon_{pre}$. Therefore the next equation is obtained

$$L_{all}(1+\varepsilon_{pre}) = 2\sum_{1}^{N/2}\left(\left(1+\sqrt{\varepsilon_{N/2+1}{}^2 + \left(\sum_{k=i}^{N/2} \frac{m_k g}{EA}\right)^2}\right) L_0 \cos\theta\right) + (1+\varepsilon_{N/2+1}) L_0 \tag{5}$$

Although the unknown parameter in this formula is the horizontal strain $\varepsilon_{N/2}$ only, which is common everywhere, it is difficult to solve the equation analytically because of the complex geometrical nonlinearity. Therefore,it is solved numerically.

**Fig. 7** shows the relation between the number of the division of the mass, and static sensitivity (in this

**Table 1** Parameters of analytical model.

| | | |
|---|---|---|
| FBG optical fiber | diameter | 125μm |
| | length | 20mm |
| | Young's modulus | 7455kg/mm$^2$ |
| Mass | Whole weight | 20g |

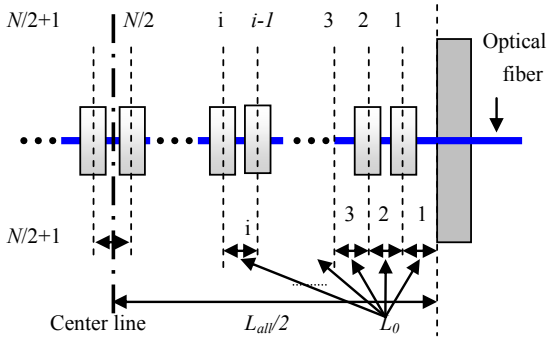


**Fig. 4** Initial state of FBG sensor without gravity.

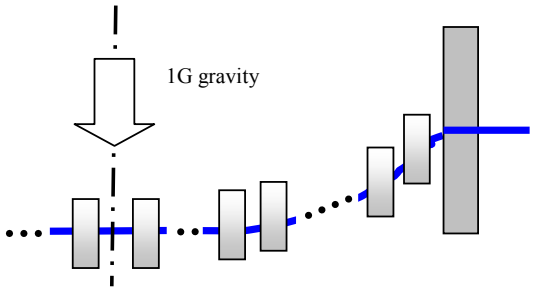


**Fig. 5** FBG sensor with gravity.

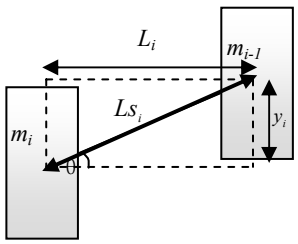


**Fig. 6** Section (i) of FBG sensor with gravity.

paper, sensitivity is defined as the strain of FBG section per 1gal(cm/s$^2$) of the input in the neighborhood of 1G), when the parameters of **Table1** are used. From this result, it is found that the reduction of the sensitivity reaches its minimum that is about 2/3 of the sensitivity achieved by the concentrated mass sensor. This sensitivity is considerd as high enough. Therefore, it may be concluded that the distributed mass sensor should resolve the problems associated with the concentrated mass sensor.

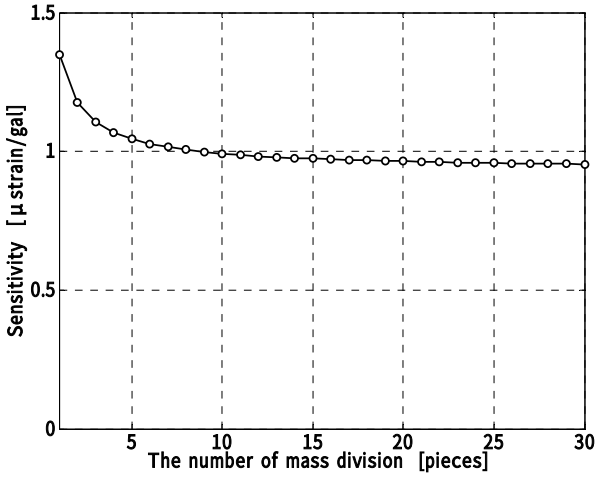


**Fig. 7** Number of division vs static sensitivity.

## 3. ANALYTICAL EXMAMINATION OF DYNAMIC CHARACTERISTICS

### (1) Derivation of linearized state equations

To investigate the dynamic characteristics of the proposed FBG vibration sensor, a stiffness matrix assuming infinitesimal displacements is derived. Then, linearized state equations are obtained.

At first, only *i*-th optical fiber is considered. The displacement in the vertical direction is obtained as

$$y_i = (1+\sqrt{\varepsilon_{N/2+1}{}^2+(\sum_{k=i}^{N/2}\frac{m_k g}{EA})^2})L_0\sin\theta \qquad (6)$$

From this equation, the static state of the optical fiber with gravity can be described. The relation between the force and resulting displacement is shown in **Fig. 8.** Because the relation exhibits strong nonlinearity, the linear spring coefficients are derived by assuming small vibration in the vicinity of equilibrium state. Thus, when the infinitesimal displacement *dy* is assumed, the incremental force at the edge of the sensor in each direction can be obtained as

$$df_{ixy}=EA\frac{\sqrt{Li^2+(yi+dy)^2}-L0}{L0}\frac{Li}{\sqrt{Li^2+(yi+dy)^2}}-EA\varepsilon_{N/2+1} \qquad (7\text{-}1)$$

$$df_{iyy}=EA\frac{\sqrt{Li^2+(yi+dy)^2}-L0}{L0}\frac{yi+dy}{\sqrt{Li^2+(yi+dy)^2}}-\sum_{i}^{N/2}m_i g \qquad (7\text{-}2)$$

$$df_{izy}=EA\frac{\sqrt{Li^2+(yi+dy)^2}-L0}{L0}\frac{0}{\sqrt{Li^2+(yi+dy)^2}}=0 \qquad (7\text{-}3)$$

and by dividing them by the displacement *dy*, the stiffness coefficient *K* is obtained. By computing the stiffness coefficients for all directions, the stiffness matrix for the section *i* can be obtained as

$$Ki = \begin{pmatrix} K_{ixx} & K_{ixy} & K_{ixz} & -K_{ixx} & -K_{ixy} & -K_{ixz} \\ K_{iyx} & K_{iyy} & K_{iyz} & -K_{iyx} & -K_{iyy} & -K_{iyz} \\ K_{izx} & K_{izy} & K_{izz} & -K_{izx} & -K_{izy} & -K_{izz} \\ -K_{ixx} & -K_{ixy} & -K_{ixz} & K_{ixx} & K_{ixx} & K_{ixx} \\ -K_{iyx} & -K_{iyy} & -K_{iyz} & K_{iyx} & K_{iyy} & K_{iyz} \\ -K_{izx} & -K_{izy} & -K_{izz} & K_{izx} & K_{izy} & K_{izz} \end{pmatrix} \quad (8)$$

By defining the displacement and velocity of each mass as state variables, the system matrix of the the sensor can be obtained easily by adding the elemental system matrices. **Fig. 9** shows the bode diagram of this sensor based on the linearized state equation. The parameters used for this evaluation are listed in **Table 1**.

From **Fig. 9**, we may conclude that the sensitivity in the vertical direction is about 10 times larger than that observed for other two perpendicular directions. This mainly attributed to the pretension and the sag arisen by gravity.

### (2) Nonlinearity of the sensor

When the response of the sensor is small enough, the linearized state equations should be good enough to represent its dynamics. However, for slightly higher levels of response, the nonlinearity of the sensor should be considered.

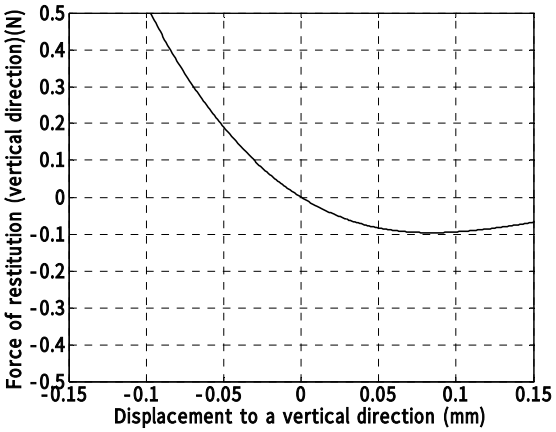


**Fig. 8** Displacement vs force.

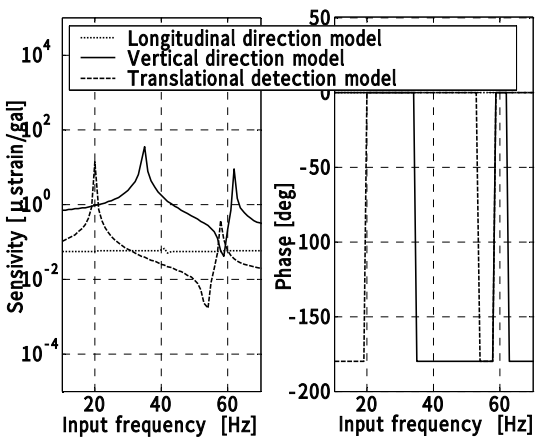


**Fig. 9** Bode diagram of the system.

#### a) Vibration in the translational direction

For the vertical direction, the linearized state equations can be formulated. However, this formulation is not applicable to the translational direction. **Fig. 9** shows the reason. Because there is no force resulting from gravity exists in the translational direction, whichever the mass moves to left or right by the inertia force, the tension arising in the optical fiber increases. In fact, it does not have any distinction between plus and minus. Therefore, only the absolute values for the displacement is associated with the strain of FBG. Therefore, it is impossible to derive simple linearized state equations for this direction. For example, when the input vibration is given to the sensor sinusoidally with 30Hz, the output, the wavelength change of reflected light, vibrates with 60Hz as shown in **Fig. 10**. Therefore, the output frequency for the translational direction is always twice higher than the input frequency.

In this paper, the transfer function in the translational direction is defined as the relation between the input and the output of the twice higher frequency of the input.

#### b) Nonlinearity due to large input

The dynamic characteristics of this sensor, when large input is applied, are considered here. For relatively large inputs, when the mass moves upward, the spring tends to be softened. On the other hand, when the mass moves downward, the spring is hardened. Thus, this sensor exhibits complex nonlinearity. Therefore, the frequency response is approximated by a hardering spring when the frequency is increased. When the frequency is decreased, the response is approximated by softening spring. The behavior is schematically shown in **Fig. 4**.

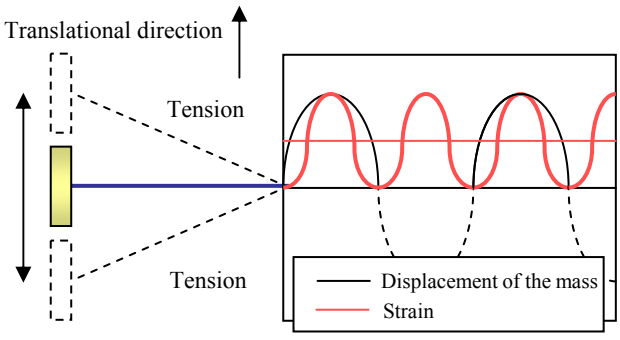


**Fig. 10** Vibration in the translational direction.

## 4. EXPERIMENTS

### (1) Optimum parameters

Based on analytical simulations, the optimum parameters were determined. At first the mass is considered. Because the FBG sensors are expected to be used in a small space, it is important to minimize the sensor. Therefore, the mass is smaller, it is better. However, to detect small vibration, although it depends on the accuracy of the interrogation system, the sensitivity target need to satisfy is 0.6 μstrain/gal. Concerning these conditions, the mass is set as 13.6g. Then, the relation between the length of the optical fiber and the sensitivity is considered. In Equation 5, using the relation that the summation of $L_0$ corresponds to $L_{all}$, all the parameters related to the length of the optical fiber can be eliminated. This fact implies that the length of the optical fiber does not affect the static sensitivity. **Fig. 12** shows the relation between the length of the optical fiber and the dynamic characteristics. From this result, it is found that by changing the length of the optical fiber, the high sensitivity frequency band can be changed arbitrarily, without decreasing the sensitivity.

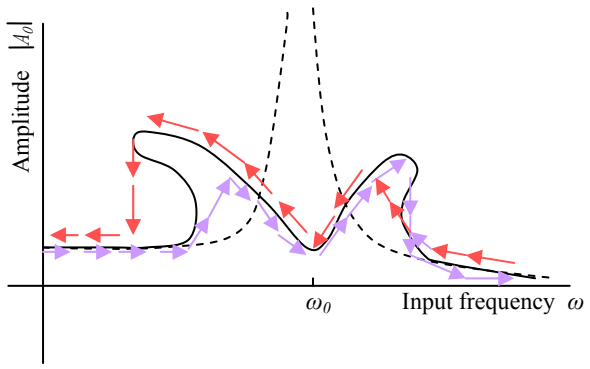


**Fig. 11** Nonlinear resonance.

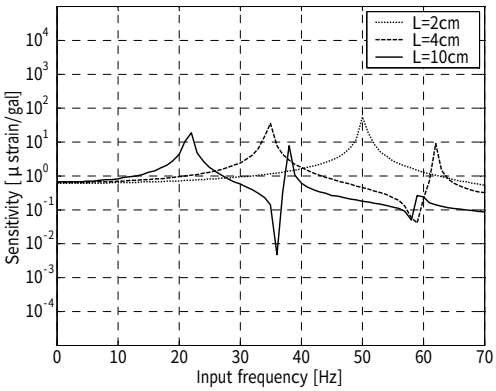


**Fig. 12** Sensitivity for different sensor length

### (2) Prototype sensor

Based on the optimum parameters, a distributed mass FBG vibration sensor was fabricated. The number of the distributed mass is 10 and attached by maintaining equal interval. The material of the mass is brass disk which is cut at the center to insert concentric rubber. By cutting the rubber to make a narrow slit, and clipping the optical fiber in it, it was possible to establish the distributed mass system that allows easy removal of the distributed mass. Because of separation and due to the rubber it does not disturb the motion of the optical fiber.

The diameter of the optical fiber is 125μm. The length of the optical fiber is either 2.2cm or 4cm. **Table 2** shows the list of parameters. **Fig. 13** shows the configuration of the mass. **Fig. 14** shows the photo of the fabricated sensor.

**Table.2** Parameters of prototype sensor.

| | | Sensor1 | Sensor2 |
|---|---|---|---|
| FBG optical fiber | Diameter | 125μm | |
| | Young's modulus | 7455kg/mm$^2$ | |
| | Length | 22mm | 40mm |
| Mass (brass part) | Diameter | 120mm | |
| | Weight | 13.6 g | |
| Mass (rubber part) | Diameter | 2mm | |

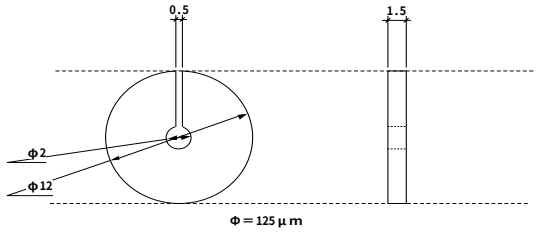


**Fig. 13** Configuration of mass element.

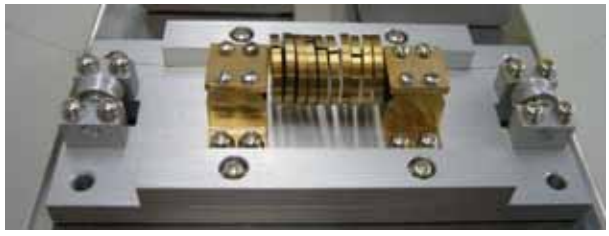

**Fig. 14** Prototype sensor.

### (3) Static performance evaluation experiment

#### a) Experimental set up

First, by watching the notch wavelength (Bragg wavelength) of the transmitted light using the optical spectrum analyzer, the strain induced by gravity is computed. In this experiment, I Sense1400 was used for interrogation.

**Fig. 16** shows the transmitted light of the sensor 2. From this result it is found that the notch wavelength shifts due to gravity. By dividing the quantity of the shift of the wavelength by the constant, 1.2 [pm/μstrain], the strain can be obtained. Assuming the relation between acceleration and the strain is similar to the analytical result, experimental sensitivity is computed. **Table 3** shows the comparison between experimental and analytical results.

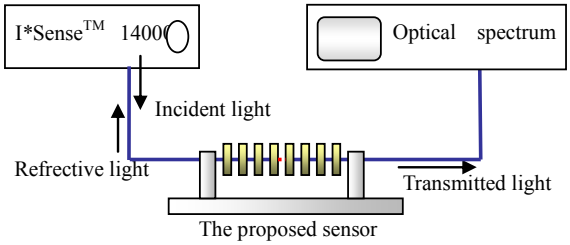


**Fig. 15** Schematic diagram of static experiment.

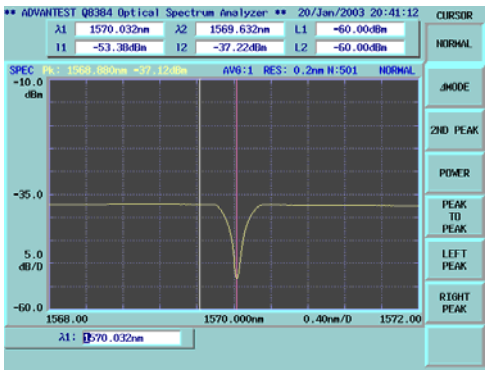

**Fig. 16(a)** Transmitted light (without gravity).

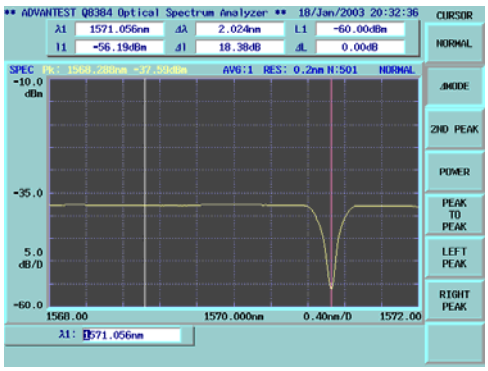

**Fig. 16(b)** Transmitted light (with gravity).

#### b) Experimental result

From the results, it is found that there is a discrepancy of about 10% between the results. The main reason of this discrepancy may be due to the error in modeling. When the strain was computed analytically, each distributed mass was assumed supported at a point of the center of the mass. But as shown in the **Fig. 14**, in the experiment, the mass isn't supported by a point but by a certain length of the fiber. It is thus anticipated to result in lower sensitivity for the prototype sensor.

### (4) Dynamic performance evaluation experiment

#### a) Experimental set up

In this experiment, the dynamic performance of the prototype sensor was investigated by shaking table experiments. The experiments were conducted for three directions. The setup was as shown below.

**Table.3** Static sensitivity

| | Shift of wavelength (nm) | Sensitivity (experiment) (μstrain/gal) | Sensitivity (analysis) (μstrain/gal) | Error (%) |
|---|---|---|---|---|
| Sensor1 | 0.952 | 0.55 | 0.67 | 18 |
| Sensor2 | 1.024 | 0.59 | 0.67 | 12 |

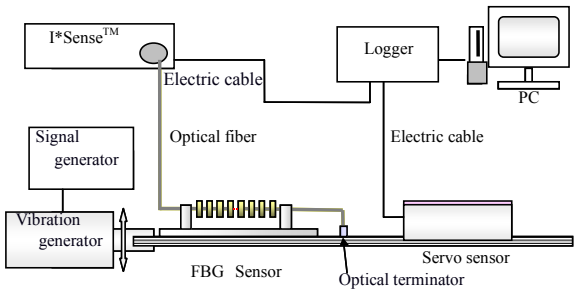


**Fig. 17** Diagram of dynamic experiment.

**Fig. 18** Shaking table experiment.

**b) Experimental result**

**Fig. 19** shows the transfer functions of this sensor. The transfer functions were obtained by considering the output of the servo sensor as the input.

From these results, it is found that the analytical results agree well with the experimental results. The sensitivity in the vertical direction is indeed large. This means that this sensor has little cross talk. The sensitivity of this sensor was found approximately 0.6μstrain/gal at low frequency. It is much larger at the resonance. This sensitivity is good enough to serve the purpose.

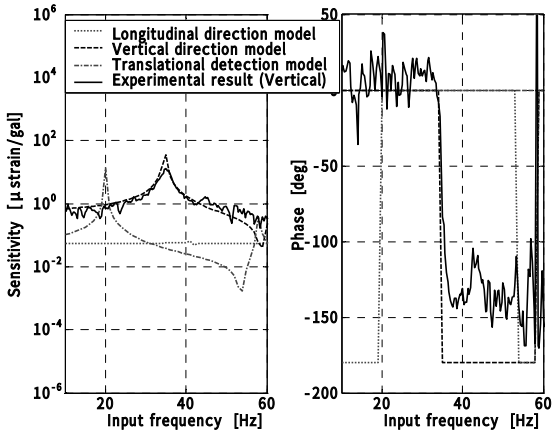


**Fig. 19(a)** Transfer functions (vertical direction).

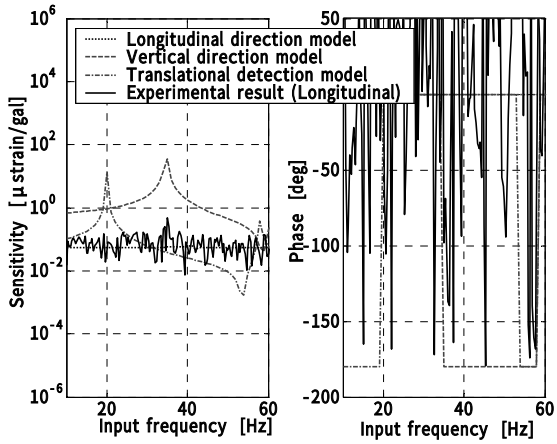


**Fig. 19(b)** Transfer functions(longitudinal direction).

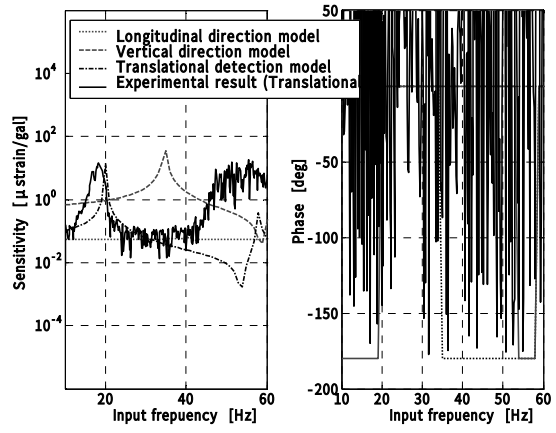


**Fig. 19(c)** Transfer functions(translational direction).

**c) Effect of fiber length**

The relation between the length of the optical fiber and the dynamic sensitivity was investigated. **Fig. 20** shows the transfer functions of the sensor 1 and sensor 2 in the vertical direction. From this result, it is found that the analytical result is correct. Due to the effect of nonlinearity of the sensor, sensor1 shows the broken peaks as shown in **Fig. 20**.

**d) Vibration in the translational direction**

**Fig. 21** shows the time-series response of the sensor in the translational direction compared to the servo sensor. From the figure, it is found that the output of the proposed sensor vibrates with twice as high frequency as the servo sensor, as stated in the 3.(2) a). This feature may be advantageous to reduce the cross talk. In addition, by using this fact to obtain two separable outputs from one sensor, we may be able to improve the accuracy of identification if appropriate signal processing techniques are used.

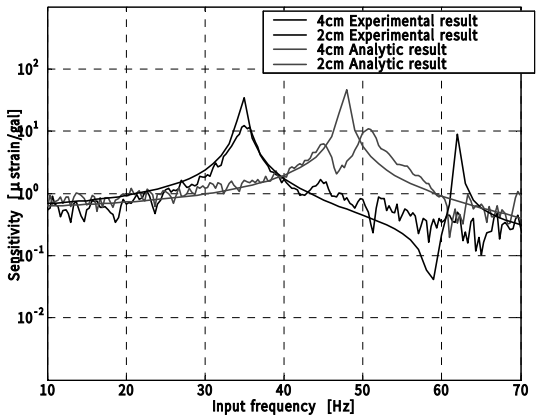


**Fig. 20** Length of optical fiber vs sensitivity.

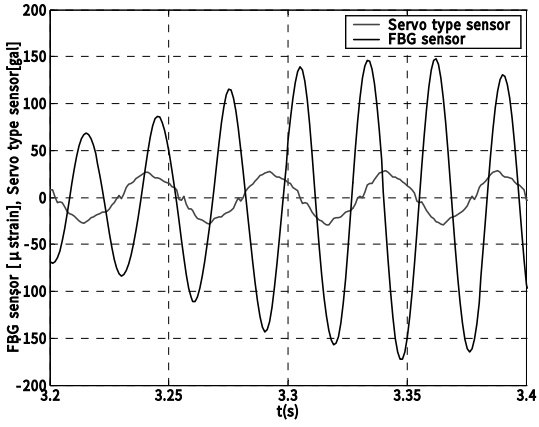


**Fig. 21** Output in the translational direction.

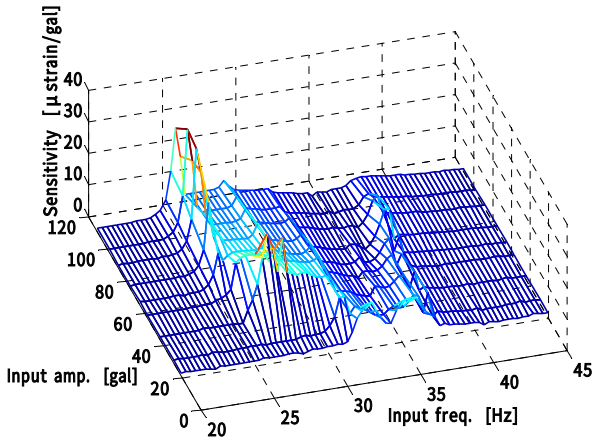


**Fig. 22** Nonlinearity of this sensor.

**e) Nonlinearity due to strong inputs**

As stated above, this sensor has complex nonlinearity for large inputs. Therefore, to examine the characteristics experimentally, sweep vibration tests have been conducted. The frequency of excitation was changed slowly from high frequency to low frequency maintaining the acceleration amplitudes of the excitation.

**Fig. 22** shows the frequency response. The horizontal axis expresses excitation frequency, whereas the vertical axis and height represent the input amplitude and sensitivity respectively. This figure shows that as the input becomes strong, the resonance frequency sifts and spreads horizontally as was expected by analytical investigations. As it does not have a sharp peak to a strong input, this sensor has such an advantage that it does not need any damping device. This feature contributes to simplify the sensor, and to reduce the costs.

## 5. CONCLUSION

A mechanism to ensure uniform strain distribution in the FBG sensor elements for vibration sensing using gravity effects was proposed. The gravity effects ensure the maximum sensitivity for the vertical direction, while keeping the minimum sensitivity for other two transverse directions so that the cross talk should be minimal. The sensitivity of the sensor can be more than 1 μstrain/ga. The extensive tests were conducted to show feasibility of FBG strain and vibration sensors. Some aspects of the sensor is summarized as follows:

1) Dividing the mass reduces the sensitivity slightly. However, it is at most 30% reduction compared with the concentrated mass.
2) The length of the fiber does not affect the sensitivity of the sensor. It only changes the resonance frequency.
3) The vibration frequency in the translational direction is doubled. This feature may be useful for identification.
4) The sensor exhibits strong nonlinearity so that it does not need addition of dampers. This feature contributes in simplifying the mechanism.

## REFERENCES

1) Todd, M. D., Johnson, G. A., Althouse, B. A. and Vohra, S. T.: Flexural beam based fiber Bragg grating accelerometer, *IEEE Photon. Techno.* Lett.10 No.11 , pp. 1605-1607,1998.
2) Mita, A. and Yokoi, I.: Fiber Bragg Grating Accelerometer for Structural Health Monitoring, *Proc. Sixth International Conference on Motion andVibration Control,* Sydney, Australia , pp. 631-636,2000.
3) Kanda, A. and Mita, A.: The FBG vibration sensor suitable for detecting a minute vibration. *Summaries of technical paper of annual meeting architectural institute of japan. B2,* pp. 959-960,2001.
4) Spammer, S. J. and Fuhr, P. L.: Temperature insensitive fiber optic accelerometer using chirped Bragg grating, *Optical Eng.*, Vol. 39 , No.8 , pp. 2178-2181,2000.
5) Brekoff, T.A.and Kersey, A.D.: Experimental demonstration of a fiber Bragg grating accelerometer, *IEEE Photon. Techno.* Lett.8 No.12 , pp. 1677-1679, 1996.
6) Kersey, A.D., Jackson, D.A. and Corke, M.: High Sensitivity Fiber-Optic Accelerometer. *Electronics Letters 18,* pp. 559-561
7) Satori, K. and Fukuji, K.: Thin optical fiber covered by polyimide resin for buried sensors, *Proceedings of smart materials symposium 2000 ,* pp. 23-26,2000
8) Thompson, J.M.T. and Stewart, H.B.: *Nonlinear Dynamics and Caos*, Wiley

**(Received February 1, 2005)**